STATUS OF TRISTAN SUPERCONDUCTING RF PROGRAM

S. Noguchi, K. Akai, M. Arinaga, K. Asano, T. Furuya
K. Hara, K. Hosoyama, A. Kabe, Yuji Kojima, Yuzo Kojima
S. Mitsunobu, H. Nakai, T. Nakazato*, T. Ogitsu, K. Saito
U. Sakamoto T. Suzuki and T. Tajima

KEK, National Laboratory for High Energy Physics
Oho-machi, Tsukuba-gun, Ibaraki-ken, 305, Japan

I. TRISTAN and Superconducting RF Program

The TRISTAN accelerator complex[1),2)], shown in Fig. 1, consists of an injector linac system, an accumulation ring (AR) and a main colliding beam ring (MR).

The injector linac system is composed of a 2.5 GeV main linac, a 200 MeV high current (10 A) linac for positron generation and a 250 MeV positron preaccelerator. These linacs are now operated with a pulse width of 2 nsec and a repetition rate of 20 pps, which is raised to 50 pps in the near future.

The TRISTAN AR is used as a beam accumulator and energy booster for the TRISTAN MR, and additionally it can be operated as an electron-positron collider and as a storage ring for the synchrotron radiation research. The electron (positron) beam of 50 mA (10 mA) peak current is injected from the main linac. The accumulation rate of positrons is now typically 5 mA/min. There are 8 RF cavity sections in two long straight sections, of which 6 sections are occupied by 11 cell APS cavities and 2 sections are used for the beam test of the superconducting cavities. The general parameters of the TRISTAN AR and MR are listed in Table I.

The TRISTAN MR was designed so that it could achieved as high energy as possible for its size, therefore it has very long straight sections for RF cavities. The normal conducting cavities, which are 9-cell APS type[3)] and have a shunt impedance of 22.5 MΩ/m, are distributed to 3 straight sections. The remaining straight section named NIKKO division, is alloted to the superconducting cavities. MR accelerated the first electron beam to 25.5 GeV on 24th of October 1986. After tuning of the accelerators, colliding beam experiments started on 10th of December at 24 GeV. The beam energy was increased to 25 GeV in May 1987, and then to 26 GeV by increasing the number of RF cavities. The maximum single bunch current achieved is 3.2 mA, which is limited by the first head-tail instability, and the total beam current of 4 bunches is 9 mA at the beginning of colliding experiments. The beam life time is about 3 hrs, which is determined by vacuum pressure at present.

The energy upgrading program was approved in 1986 and the construction of 32 5-cell superconducting cavities and a 4.5 KW helium refrigerator system started. It is expected that the accelerating field and the Q value are better than 5 MV/m and 1×10^9, respectively. The present schedule of the program is shown in Table 2.

---

* Now at Laboratory of Nuclear Science, Tohoku University, Mikamine, Sendai, Japan

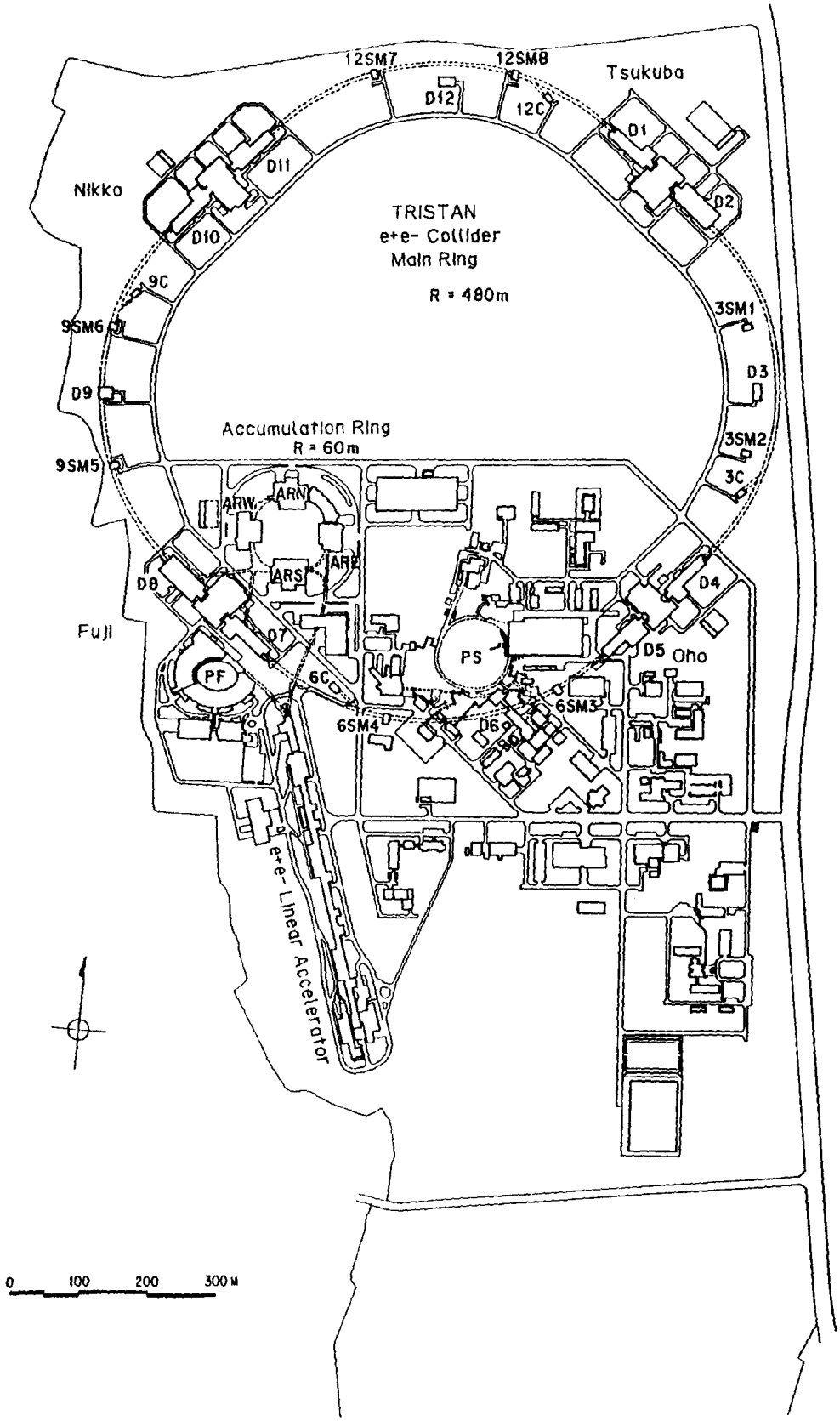

Fig. 1 Accelerators in the KEK Site.

Table 1 General Parameters of AR and MR

	AR	MR
RF frequency	508.58 MHz	508.58 MHz
Harmonic number	640	5120
Circumference	377 m	3018 m
Length of long straight section	2×19.45 m for experiment 2×19.05 m for RF cavities	4×194.35 m
Length of cavity sections	8×3.7 m	(3×40+24)×5.47 m
Bending radius	23.173 m	246.53 m
Bending field	0.86 T/6 GeV	0.406 T/30 GeV
Energy loss per turn	4.9 MeV/6 GeV	290 MeV/30 GeV
Over voltage ratio for 24 hrs life	2.09/6 GeV	1.31/30 GeV
Momentum compaction factor	0.013	0.0015
Synchrotron oscillation frequency	35 KHz/6 GeV	9.98 KHz/30 GeV
Natural bunch length	1.8 cm/6 GeV	1.17 cm/30 GeV
Natural energy spread	1.1×10^{-3}/6 GeV	1.6×10^{-3}/30 GeV
Injection energy	2.5 GeV	6.5 - 8 GeV
Maximum energy	8 GeV	> 33 GeV
Maximum beam current achieved	90 mA/single bunch	3.2 mA/one bunch 9.5 mA/4 bunch
Number of 1 MW klystrons	2	30

Table 2 Energy Upgrading Schedule

	Present	Oct. 1987	Oct. 1988	April 1989	?
No. of N.C. Cavities 9-cell APS (1.2 MV/m)	80	104	104	104	64
No. of S.C. Cavities 5-cell Spherical (5 MV/m)	0	0	16	32	64
Total RF Voltage (MV)	255	331	451	571	684
Max. Beam Energy (GeV)	27.1	28.9	31.3	33.3	34.9
No. of 1 MW Klystrons	20	26	28	30	24

We have already measured two MR 5-cell cavities, and hereafter, we must measure at least two cavities per month and accomplish the assembling them in one horizontal cryostat and the high power test. The other main work, the preparation of the beam test of two 5-cell cavities in AR, is also progressing. It is scheduled in the next month.

II. Superconducting RF System

II.1 High Power and Low Level RF System

Fig. 2 shows a block diagram of the superconducting RF system for MR. The main difference from the normal conducting system is that one krystron drives 8 superconducting cavities instead of 4 cavities. So

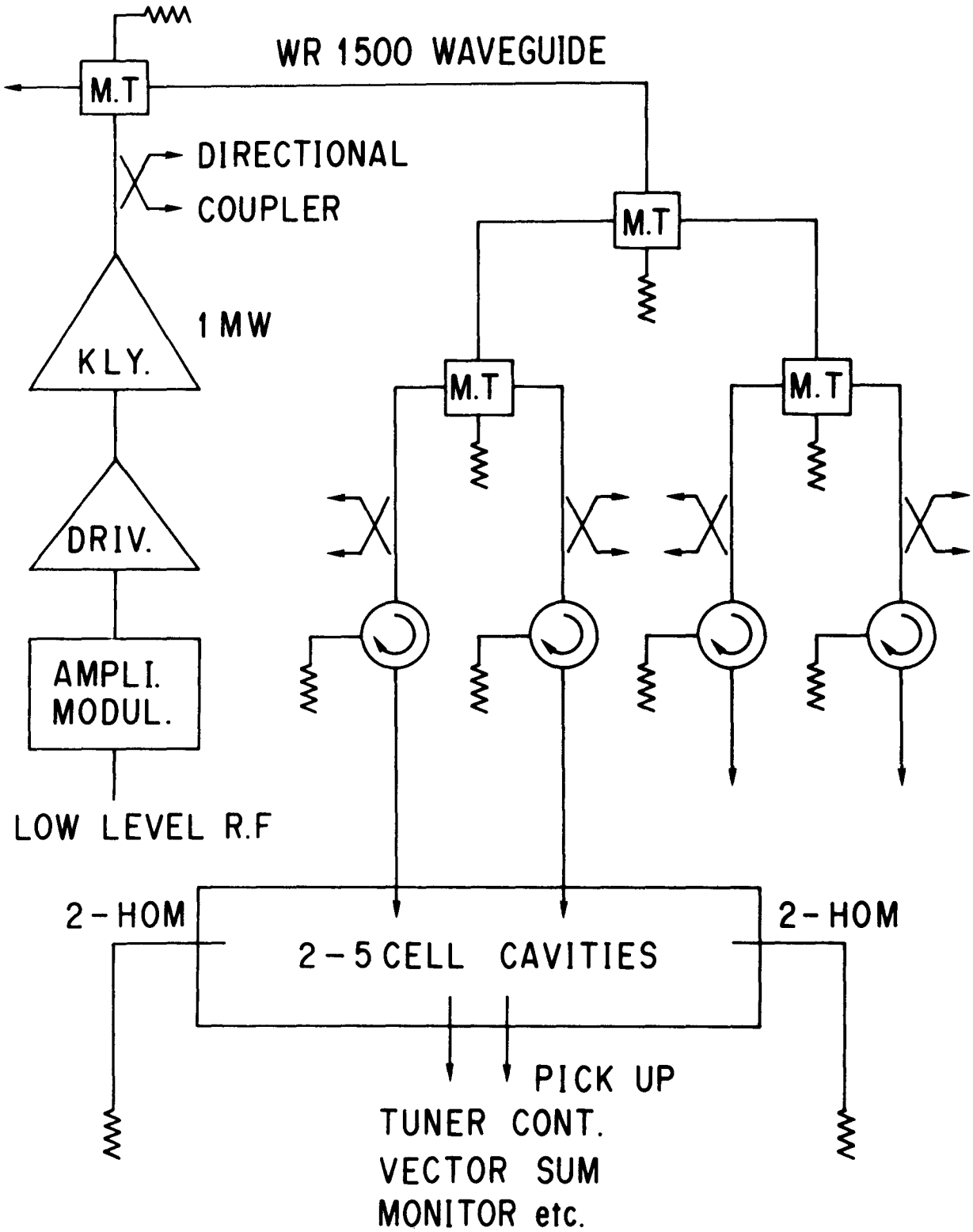

Fig. 2 RF System for the Superconducting Cavities.

the maximum accelerating field is limited by the worst cavity among 8 cavities, and the system should be used stably, because if one krystron is switched off the beams might be lost.

The output power from a 1 MW krystron, which is supplied by Toshiba and/or Valvo, is halved three times by magic-tees and is fed to 8 superconducting cavities through 150 KW circulators. The available power for one cavity is 110 KW at most, which corresponds to the accelerating field of 6 MV/m with the design total beam current of 16 mA.

The monitor signals are used for the cavity phase lock and the vector sum of 8 cavities is used for the voltage control and the phase control between other RF systems.

The low level RF system is almost the same one as used for the normal conducting cavities[4], but few modules like phase detectors are improved in consideration of wide dynamic range of the superconducting cavities.

II.2 Cavity

The details of the fabrication, the surface treatment and the vertical test are reported by T. Furuya in this workshop. Only the brief description is given here. The principal parameters of the MR cavities are listed in Table 3, and the MR 5-cell cavity is shown in Fig. 3.

Table 3 Principal Parameters of the MR Cavities

Frequency	508.58 MHz
Effective Length	1.473 m
R/Q	600 Ω
Geometrical Factor	269 Ω
Cell to Cell Coupling Coefficient	1.5 %
Surface Peak Electric field/Eacc	1.97
Surface Peak Magnetic field/Eacc	40.6 Gauss/MV/m
No. of Beam Pipe HOM Couplers	2
Q value of the Beam Pipe Input Coupler	1×10^6
RRR	100 ∿ 120

Two 5-cell cavities are installed in one cryostat. They are separated by two half λ beam pipes where the input couplers are set. The coupling coefficient of the accelerating mode between two cavities is only 1×10^{-9}, so the equivalent circuit calculation gives 1×10^{-3} for the interference of the accelerating field with a loaded Q of 1×10^6. The MR cavities are different at two points from the AR cavities shown in Fig. 4. Firstly they are made by hydro-forming instead of by spinning, and secondarily the HOM couplers on the equator of the end cell are eliminated because of the smaller beam current.

The standard procedure for the MR cavities is as follows.[5]

1. hydro-forming of half cells from Nb sheets of 2.4 mm thick
2. buffing and dipping in HCl solution
3. electron beam welding (EBW) from the outside and grinding of seams from the inside
4. first electropolishing (EP) of about 80 μm
5. annealing in a box of titanium sheet
6. tuning of the frequency and the field distribution by the permanent deformation

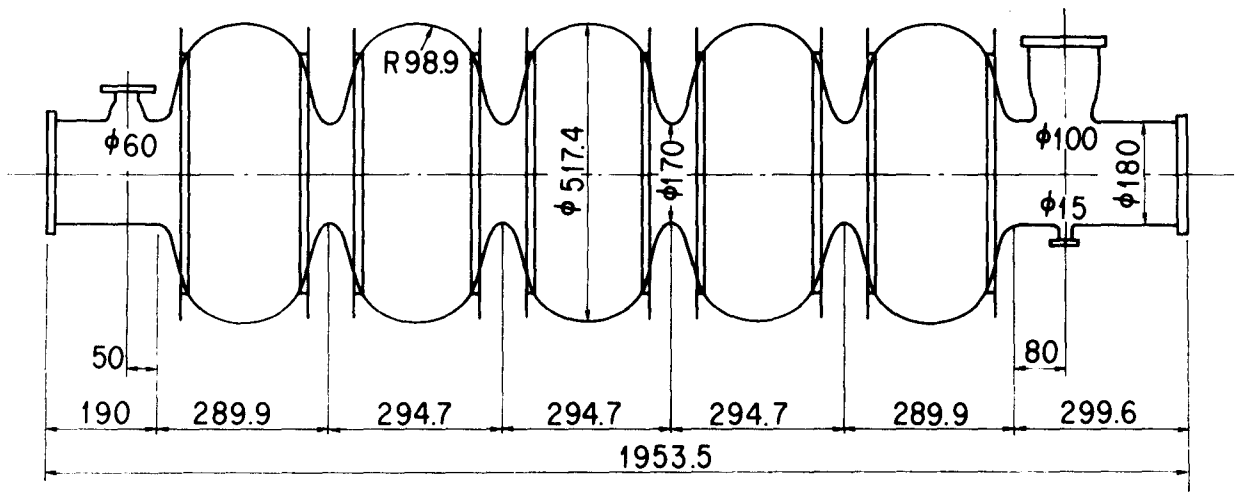

Fig. 3 MR 5-cell Cavity.

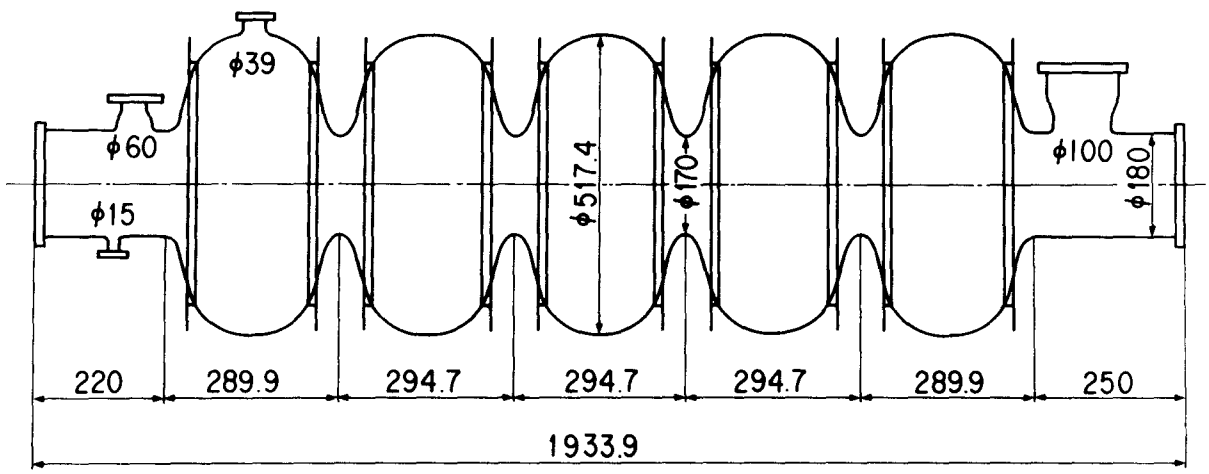

Fig. 4 AR 5-cell Cavity.

7. final electropolishing of about 5 μm
8. rinsing with the demineralized pure water and H_2O_2 of electric grade and ultrasonic
9. final rinsing with the demineralized (18 MΩ·cm), filtered (0.2 μm) and ultraviolet sterilized pure water

The results of the vertical test of two MR cavities are shown in Fig. 5 with other results of two AR cavities and two single cell cavities measured after the last beam test of the prototype AR cavity[6]. These are all first cooldown results. The excellent performance of MR cavities is due to use of the fresh EP solution and improvements of the final rinsing. On the contrary, the EP solution used for the AR cavities was probably contaminated by using several times for the first EP. So in the coming surface treatment, the fresh EP solution is used for the final EP of 4 cavities and the used for the first EP of the next 4 cavities by adding HSO_3F and H_2O appropriately to maintain the proper concentration of HF.

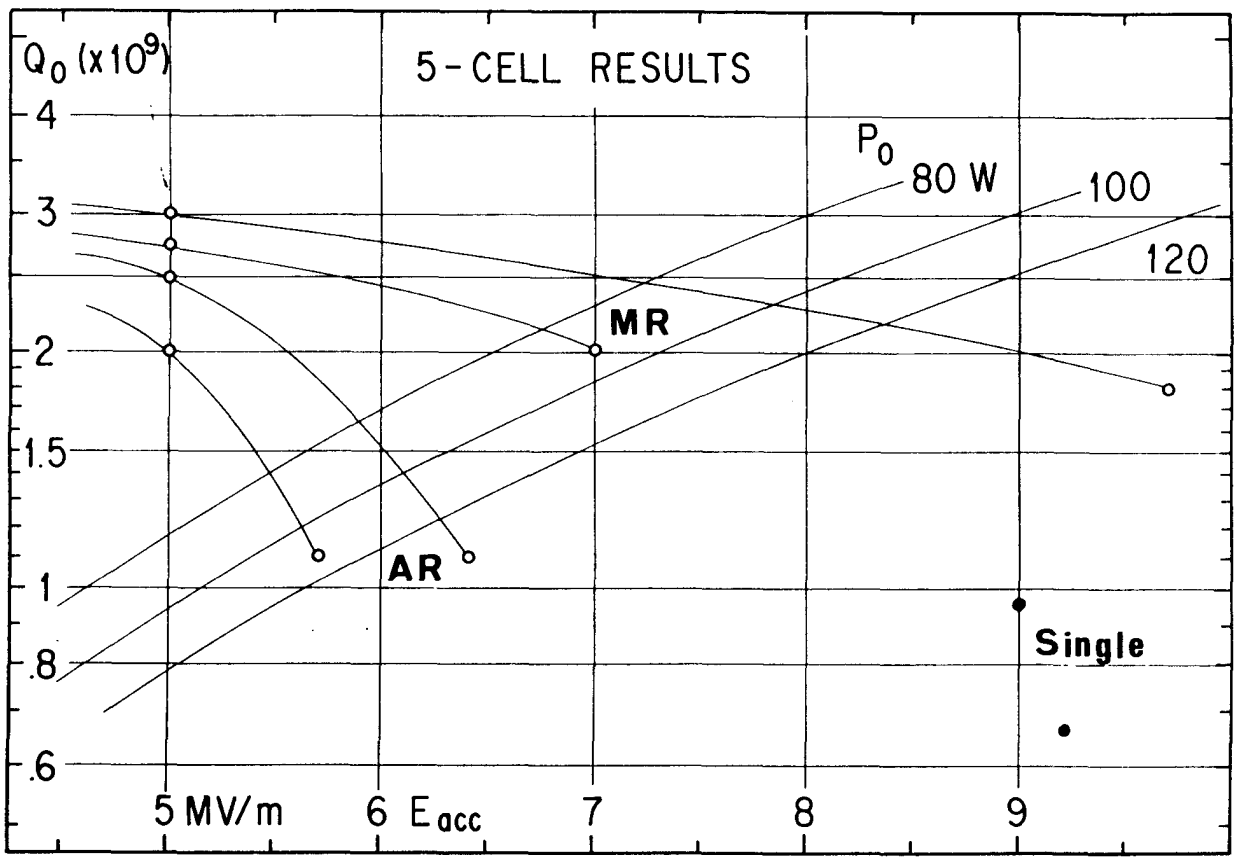

Fig. 5 Recent Results of Vertical Measurements.

II.3 RF Input Coupler and Monitor Coupler

The input coupler for the MR cavities is shown in Fig. 6. Almost the same couplers are used for two AR cavities. The input coupler consists of a coupling port on a beam pipe, a 50 Ω coaxial line, a coaxial disk ceramic window and a doorknob type transformer.

The inner conductor has a diameter of 52 mm and made of 1 mm thick OFHC copper pipe. The outer conductor is made of 2.5 mm thick stain-

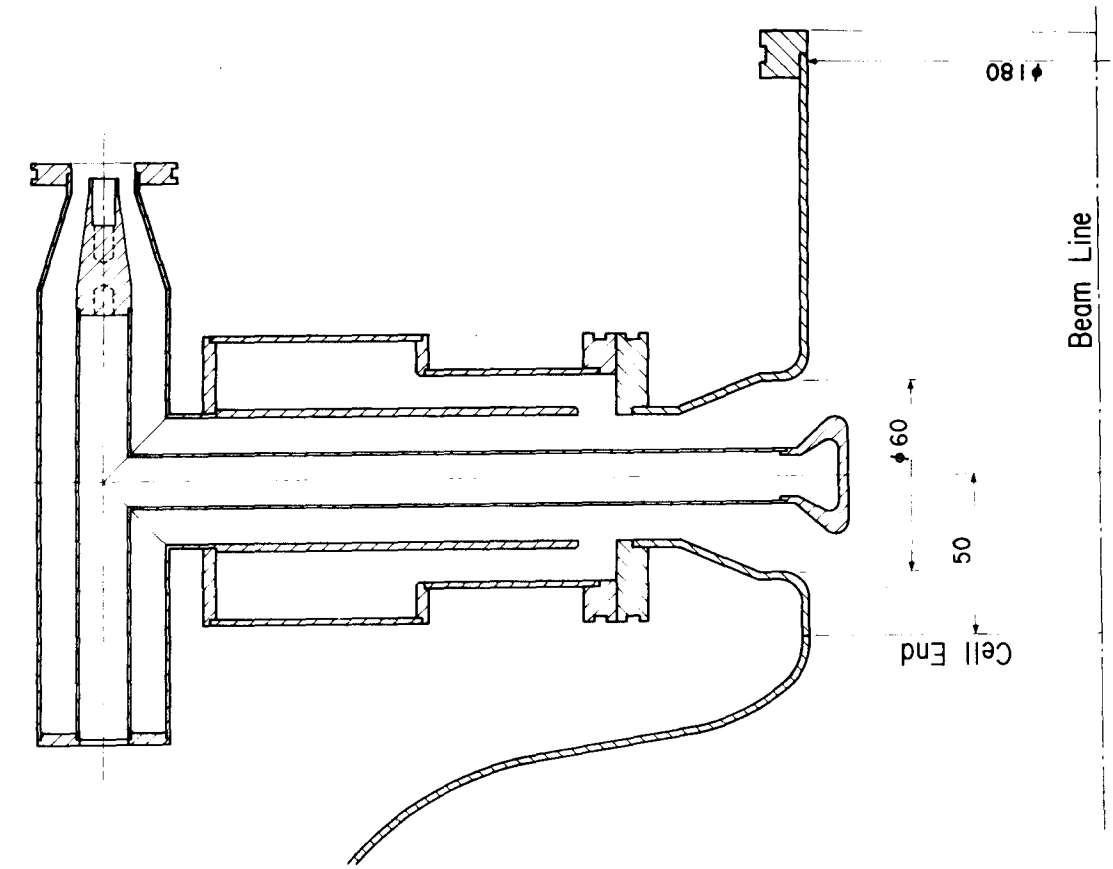

Fig. 7 Beam Pipe HOM Coupler.

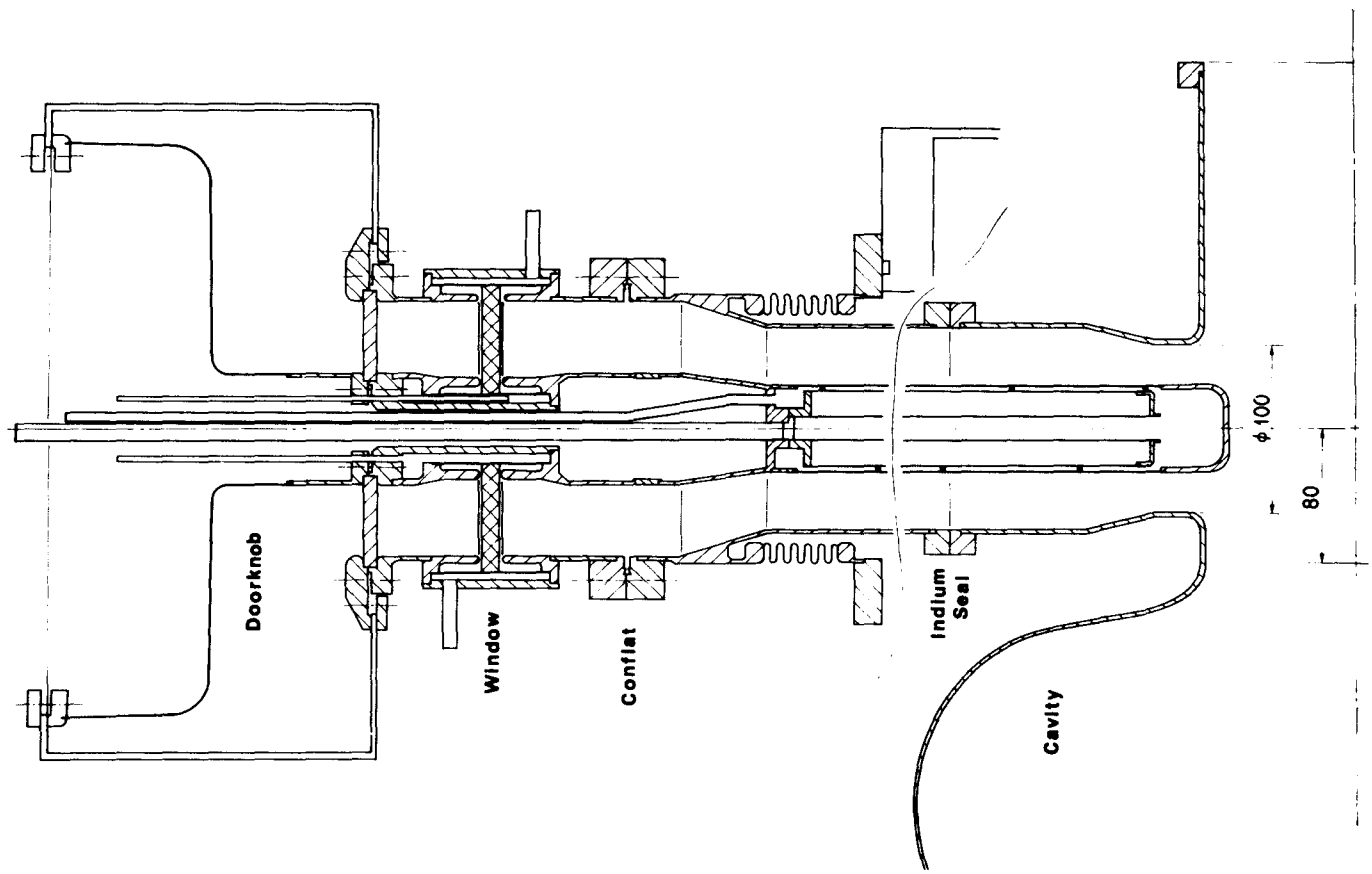

Fig. 6 Input Coupler.

less steel. These are copper plated by 30 μm. The inner conductor is projected into the beam pipe by 14 mm giving the coupler Q value of 1×10^6, and is cooled by water. The measurements on the prototype 5-cell cavity showed that the heat radiation from the inner conductor could be neglected and the RF loss at the coupler tip was small enough, about 8 W at the field level of 3 MV/m. The connection of the outer conductor to the input port flange is done directly with a indium ribbon. No excessive heating was observed up to 82 KW of the totally reflected power in the last measurements.

The ceramic window is made from alumina of 95 % purity and has a size of $170 \times 42 \times 10$ mm^3. It is cooled by water and no coating is done. VSWR of this part is about 1.15. This is the most important part in the actual aplication of large scale, therefore the input couplers will be tested at least up to the power level of 50 % higher than the maximum operating power before mounting them to the cavities.

The doorknob is made of 1 mm thick copper sheet and very flexible. VSWR of this transformer is less than 1.1 for 508 MHz, but the band width is narrow and no HOMs can be extracted.

The monitor coupler is set just below the input coupler. It is a stainless steel rod of 4 mm in diameter and the Q value is adjusted to about 3×10^{11}. The N-type coaxial ceramic connector, which is welded to a mini-conflat flange, is located in the insulation vacuum and not cooled.

II.4 HOM Couplers

The beam pipe HOM coupler made of Nb is shown in Fig. 7. The MR cavities have two beam pipe HOM couplers on the other side from the input coupler and they are inclined by ± 45°. The measured coupling of these couplers for the HOMs of the frequency below 1 GHz are summarized in Table 4 together with the coupling of the equator HOM couplers and some parameters of HOMs. R/Q values are calculated by SUPERFISH for longitudinal modes and by URMEL for transverse modes. The coupler tips are projected by 10 mm for the equator couplers and by 15 mm for the beam pipe couplers, respectively.

The projection of the coupler tips for the MR cavities is increased to 20 mm, which gives the improvements of couplings by a factor of 2. So we can expect that the impedance of longitudinal modes are less than 1 MΩ and the transverse impedance are less than 30 MΩ/m. Because the electron and the positron bunches are out of phase for these HOMs in most cases, dumping is small enough. For example, the loss by the 0-mode of TM_{011} family is 100 W with a electron or positron current of 10 mA.

Considerable unbalance of couplings between 0 and 1/5 π modes of TM_{011} family is due to asymmetry between two end cells. The HOM end cells of these two AR cavities are formed by three parts in order to make the coupling ports. This caused a slight change of geometry and pushed the field distribution of these two modes into an opposite end cell each other. The computer calculation shows that these modes are strongly excited in end cells and the field distribution is very sensitive only to the dimensions around the equator and not to those of the tapered section. Therefore the HOM end cell of the second AR cavity (AR #3) is shortened by 1 mm at the equator straight section. This shortening is adjusted to 0.3 mm for the MR cavities in consideration of the R/Q values of two modes, which are not so sensitive to the field asymmetry.

Table 4 HOM Properties of the AR Cavities

		AR #2 Cavity				AR # 3 Cavity			
				Qext of HOM Couplers				Qext of HOM Couplers	
Mode	R/Q (Ω/m)	f_0 (MHz)	Polarization	2 × Cell (× 10^4)	2 × Beam Pipe (× 10^4)	f_0 (MHz)	Polarization	2 × Cell (× 10^4)	2 × Beam Pipe (× 10^4)
TE_{111}									
1/5π	5.90	649.52	- 45°	80.1	159	649.64	- 45°	79.3	137
		649.73	+ 45°	66.9	150	649.77	+ 45°	61.6	89.3
2/5π	10.0	659.22	Horizontal	18.9	26.9	659.59	- 45°	24.2	33.7
		659.49	Vertical	20.1	29.5	659.77	+ 45°	20.5	23.6
3/5π	350	674.03	Horizontal	12.6	14.0	673.68	Horizontal	12.1	12.9
		674.34	Vertical	12.1	13.8	673.78	Vertical	12.0	12.5
4/5π	450	690.22	Horizontal	11.2	8.45	689.90	Horizontal	11.3	5.94
		690.56	Vertical	11.7	8.82	690.13	Vertical	11.7	6.70
π	120	706.46	Horizontal	18.5	4.85	706.49	Horizontal	17.3	3.68
		706.90	Vertical	18.5	4.48	706.68	Vertical	16.5	3.68
TM_{110}									
π	15.0	717.64	Horizontal	19.4	5.71	717.83	Horizontal	54.0	4.02
		717.99	Vertical	66.8	5.08	717.96	Vertical	60.7	10.6
4/5π	170	731.00	Horizontal	1520	9.44	730.53	+ 45°	6270	11.4
		731.21	Vertical	2630	10.6	730.64	- 45°	7540	9.24
3/5π	340	739.17	Horizontal	101	18.2	739.52	- 45°	144	17.8
		739.35	Vertical	115	19.2	739.61	+ 45°	118	14.4
2/5π	93.0	744.10	Horizontal	81.8	49.1	744.13	- 45°	108	36.9
		744.12	Vertical	76.6	36.4	744.22	+ 45°	88.7	29.0
1/5π	0.38	746.23	Vertical	225	161	745.90	- 45°	158	77.4
		746.31	Horizontal	225	206	745.98	+ 45°	192	90.1
TM_{011}	(Ω)								
4/5π	0.2	919.29		13.2	51.2	919.04		10.4	41.2
3/5π	1.2	925.32		3.18	10.6	925.96		3.32	12.2
2/5π	27	934.59		1.84	5.33	933.47		2.10	6.79
1/5π	56	943.66		0.294	0.927	942.05		1.60	4.99
0	103	945.61		7.42	23.6	943.81		0.284	0.892

The property of the coaxial filter is shown in Fig. 8. The frequency of the second stop band is varied in two HOM couplers by changing the diameter of both inductive and capacitive part and length of T stub so that there is no stop band as a whole. A typical tolerance is ± 0.1 mm, which corresponds to an error of ± 1 MHz for the frequency of the main stop band. Fine tuning within 1 MHz is possible by squeezing and controlling the amount of chemical polishing. The coupling Q values for the accelerating modes of two AR cavity are greater than 1×10^{10}.

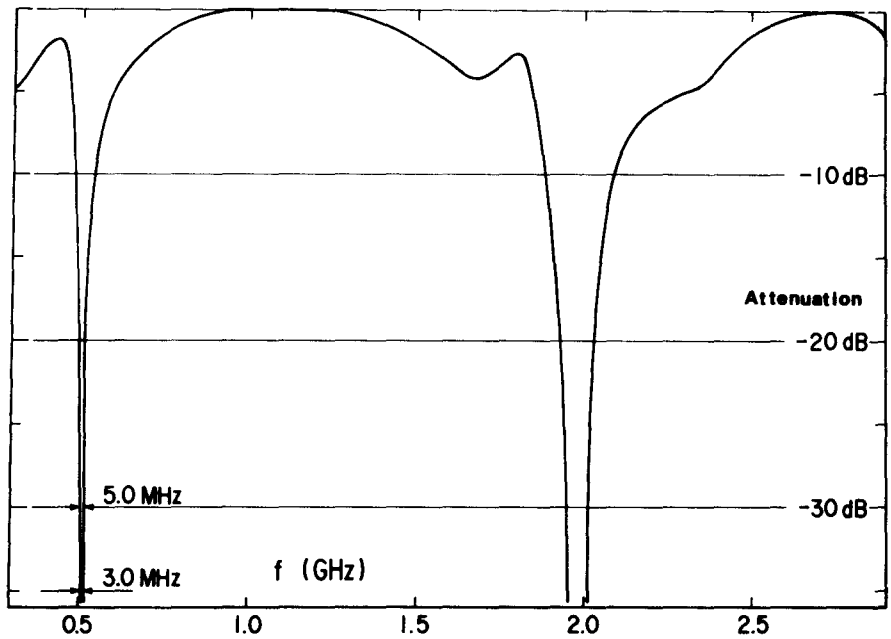

Fig. 8 RF Property of the Coaxial Filter.

II.5 Tuner

The same type tuning system, shown in Fig. 9 is used for the AR and MR cavities. It consists of a rough mechanical tuner, a fine piezo electric tuner and a lever arm to magnify the tuning range by a factor of 2. The mechanical tuner is a set of a stepping motor, gears and a jack volt, and changes the length of the cavities by 0.21 μm/pulse. The piezo tuner is a stack of 60 layers of a piezo element which is 1 mm thick and 32 mm in diameter. The stroke of the piezo tuner is about 100 μm with a rated voltage of 1600 V. The maximum permissible load is at least 2 ton, and this ensures the wide tuning range of about 10 mm. The tuning sensitivity of the cavities is about 75 KHz/mm.

The dynamic responce of the tuning system was measured using one of the AR cavities. In the measurements, the frequency of the signal generator was modulated by a depth of a half band width, 250 Hz, with various modulation frequency. By tuning the gain and the filter time constant of the phase lock loop, the oscillation of the field level with a frequency up to 10 Hz was completely suppressed as is shown in Photo. 1. This responce frequency will be improved by further tuning or use of other type of filter.

The characteristic feature of this system is that it resonates at about 50 Hz. The first Fourier analysis of the vibration shows that

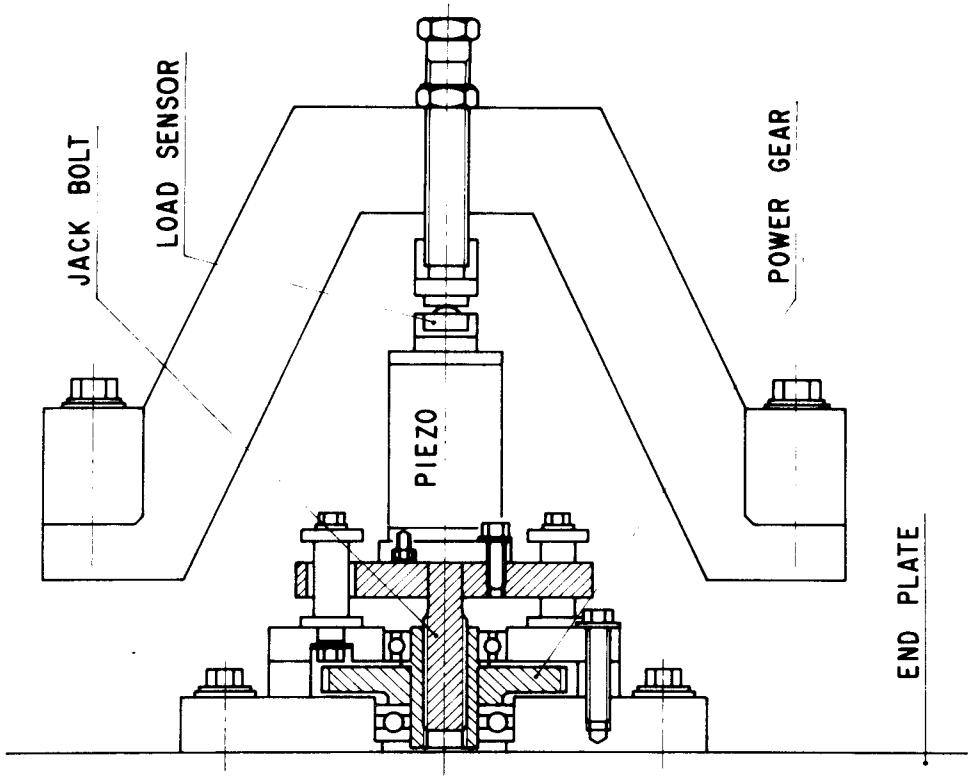

Fig. 9 Dynamic Frequency Tuning System.

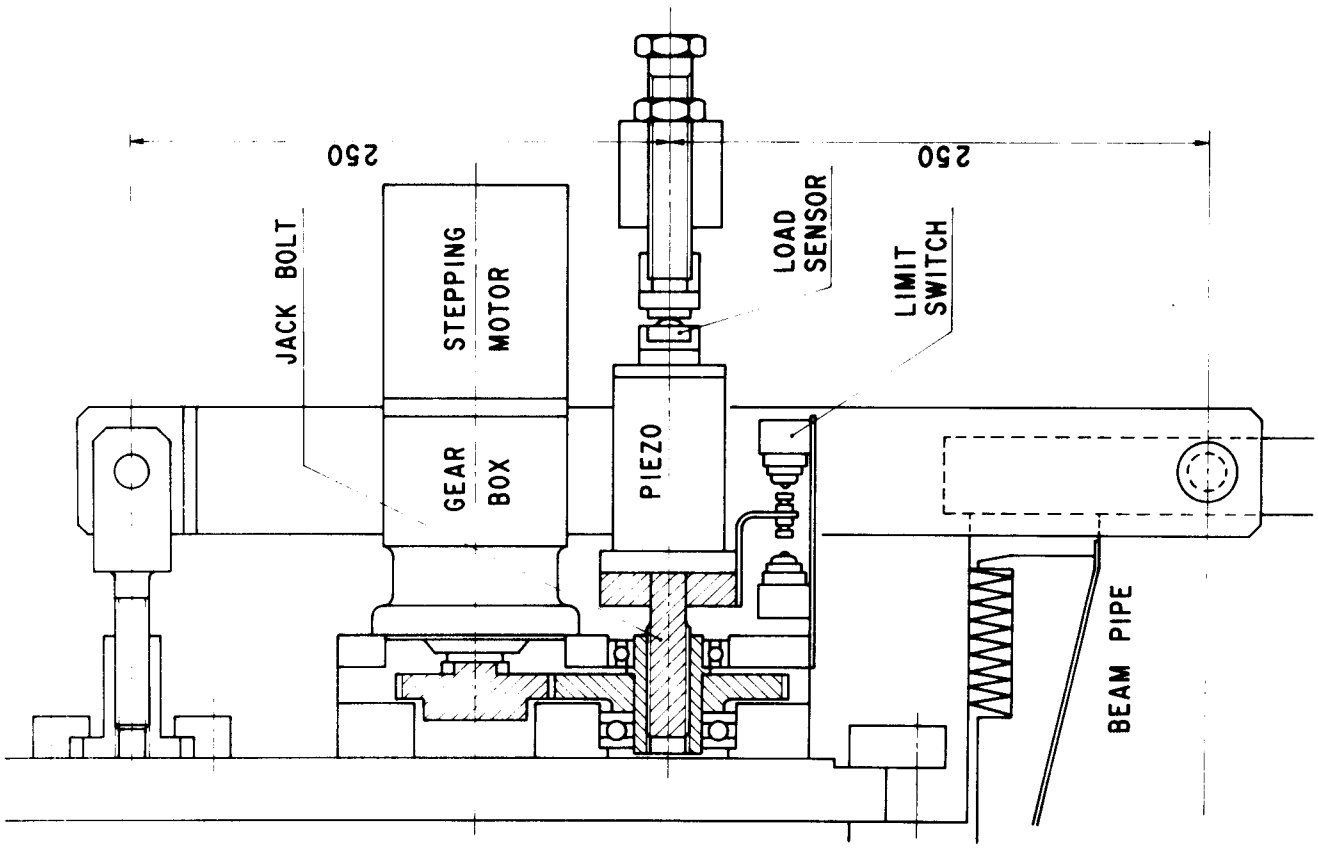

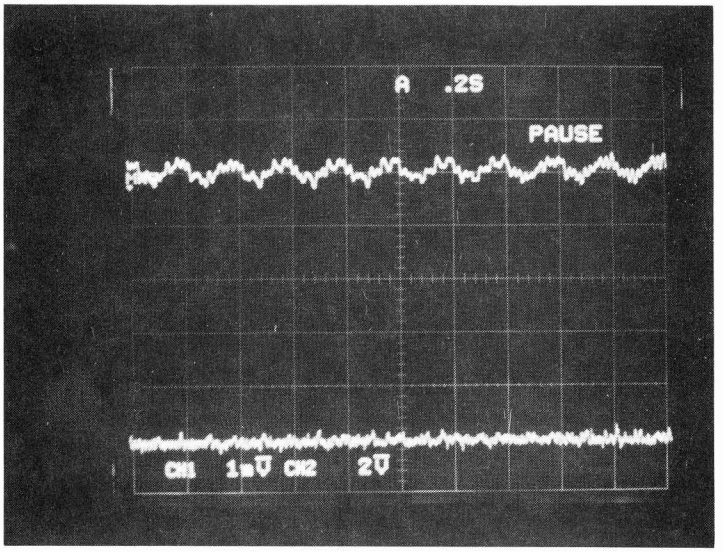

Ground

Phase : 40 °/ div.

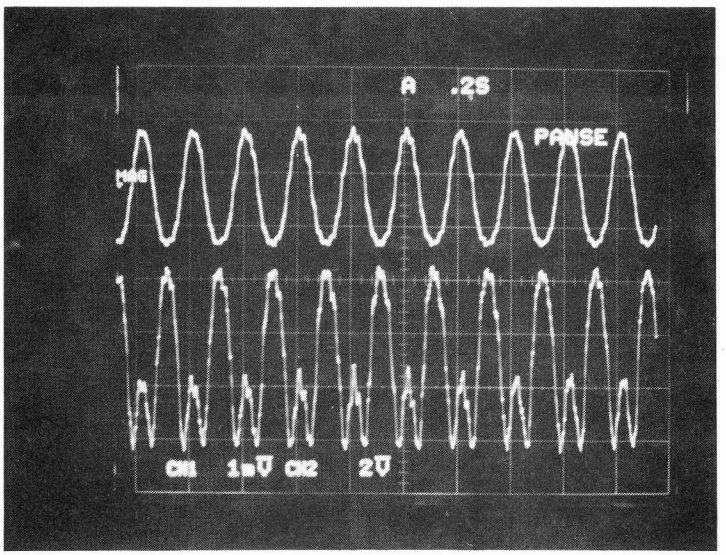

Phase

Level

Photo. 1 Field Level and Phase of a AR Cavity with a Phase Lock Loop (Upper) and without (Lower).

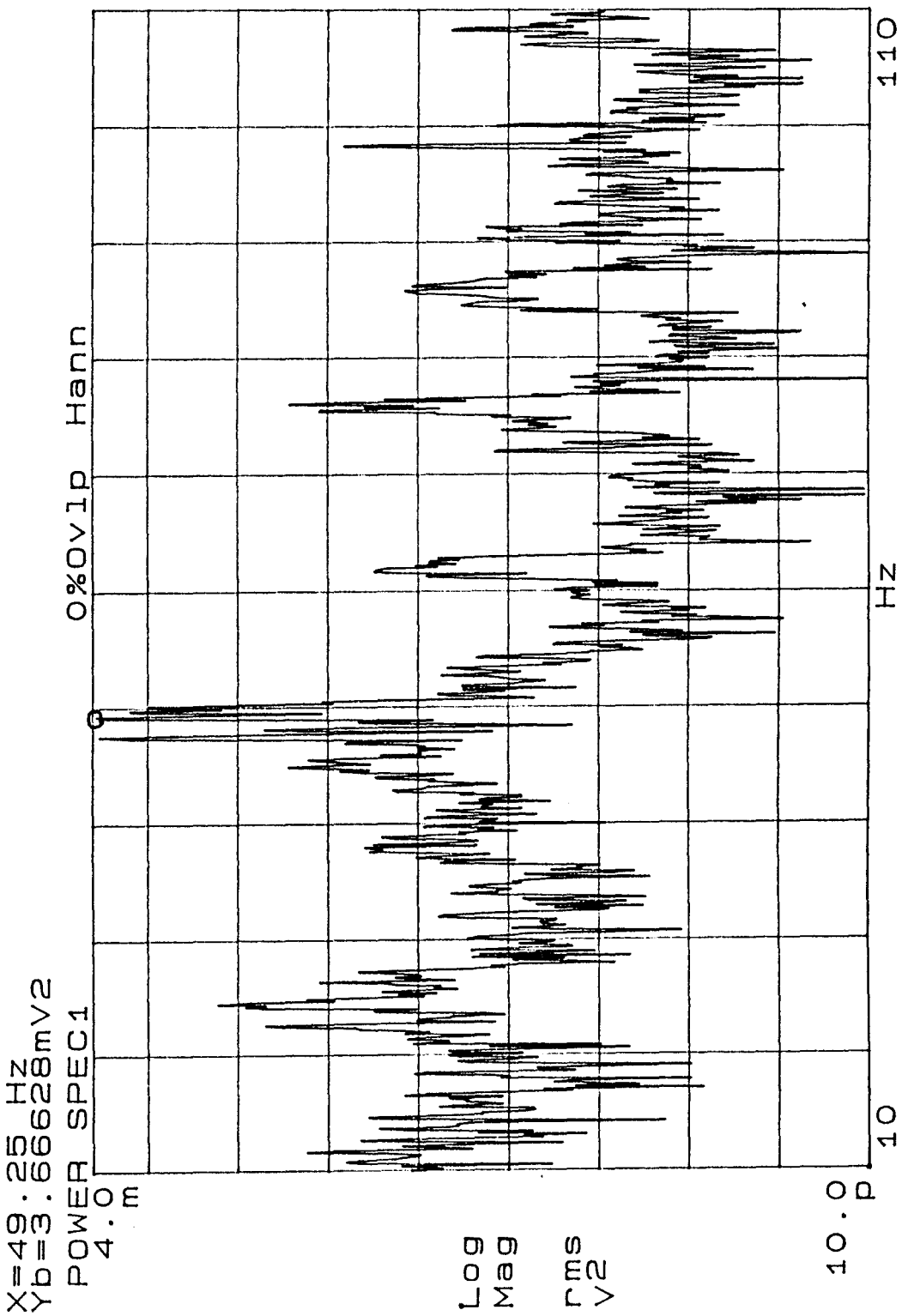

Fig. 10 FFT Analysis of the Mechanical Vibration.

the mechanical part, probably the cavity itself, has a resonance at 50 Hz as is shown in Fig. 10. Then if this frequency component in the vibration is large, the system must be modified.

The dumping time constant of sudden frequency change like due to beam injection is 50 msec and wide range responce speed is about 5 KHz/sec.

III. Cryogenic System

III.1 Cryostat

Fig. 11 and Fig. 12 show the horizontal cryostat for the AR and MR cavities, respectively. Two improvements are performed to the MR cryostat. Firstly the diameter of the He vessel is reduced to 70 cm from 80 cm for the AR cryostat, which is due to the elimination of the equator HOM couplers. Secondarily all N-type coaxial ceramic connector used for HOM and monitor couplers are moved into the insulation vacuum, and they are not cooled. But this imposes the severe tolerance on the construction of cavities, couplers and on the assembling of the cryostat.

The He vessel is surrounded by a magnetic shield, which is a 2 mm thick Permalloy and reduces terrestrial magnetism to less than 40 m Gauss. A 1 mm thick copper LN_2 shield with brazed-on copper piping is supported by the magnetic shield. These are surrounded with 20 layers of superinsulation from in and outside. The static heat load is about 13 W for the AR and 28 W for the MR cryostat, of which a half is due to the input couplers.

III.2 Refrigeration system[7)]

A flow diagram of the He refrigeration system for the MR cavities is shown in Fig. 13. The system consists of a compressor system, a cold box, a 12,000 ℓ He dewar and a He gas recovery system. The design refrigeration power of the system is 6.5 KW at 4.4°K, but at the first stage, where compressors C_5 and C_6 are not incorporated, the refrigeration power is estimated to be 4.5 KW. The total static heat load, which is sum of 16 cryostats, 380 m long transfer line (1.1 W/m), cold valves and bayonet joints, is about 1 KW. The estimated cooldown time from the room temperature to 4.4°K is about 3 days and is about one day to fill the liquid He by 900 ℓ in each of 16 He vessels.

In order to suppress the pressure fluctuation due to the change of RF level during energy ramping, heaters in the He vessels might be used.

IV. Beam Test

Up to now, we have performed two beam tests in AR using a 3-cell cavity[8)] and a 5-cell cavity. The next beam test is scheduled in October for one week. The goal of this beam test is to demonstrate the stable operation with high field, high beam current and with two cavities. For this purpose, followings should be studied.

1) Beam-cavity interaction and effect of HOM couplers
2) Ability of the input coupler
3) Ability of the tuner including the cavity phase lock loop and responce to sudden chande of beam loading
4) Requirements for heater compensation

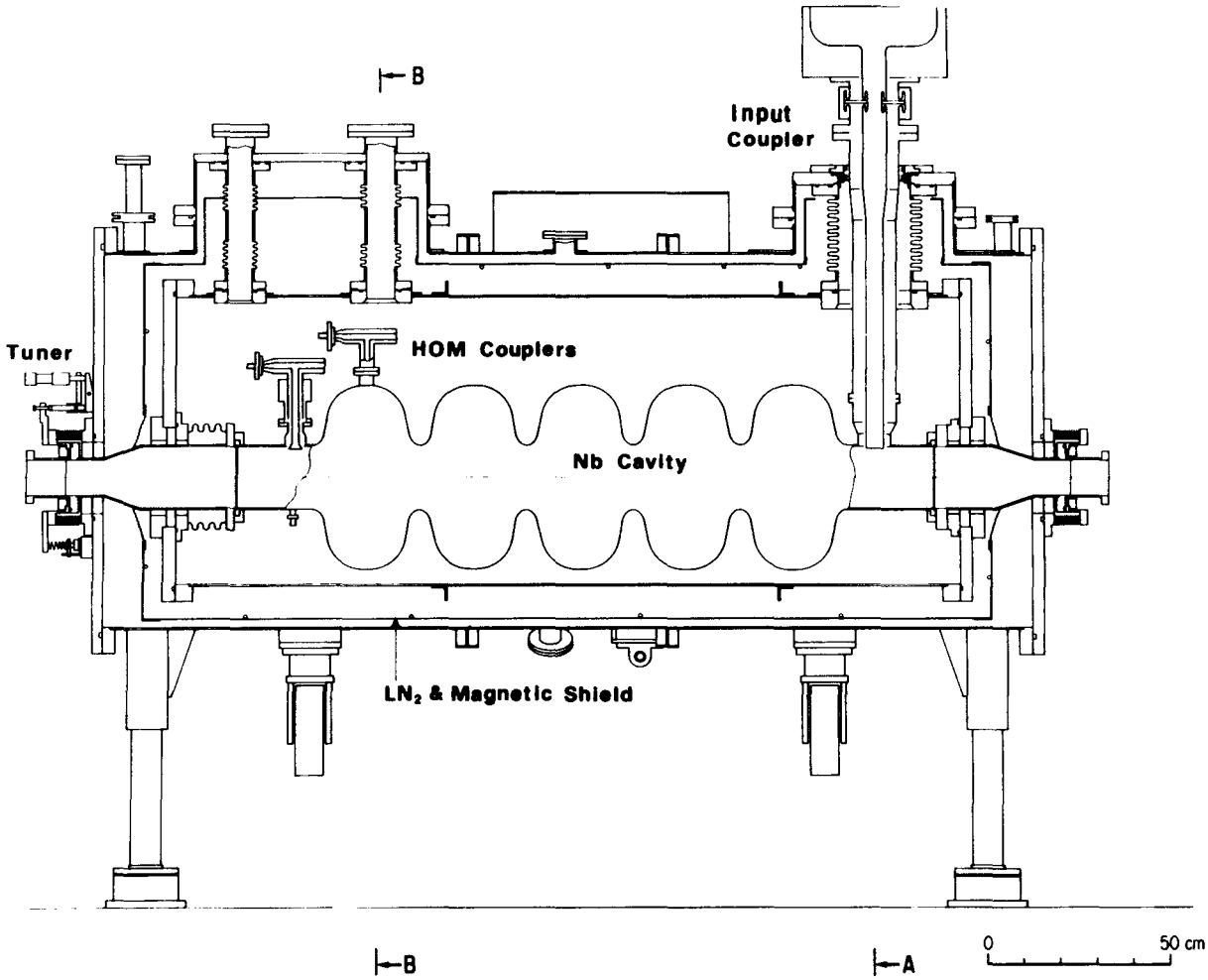

Fig. 11 AR Horizontal Cryostat.

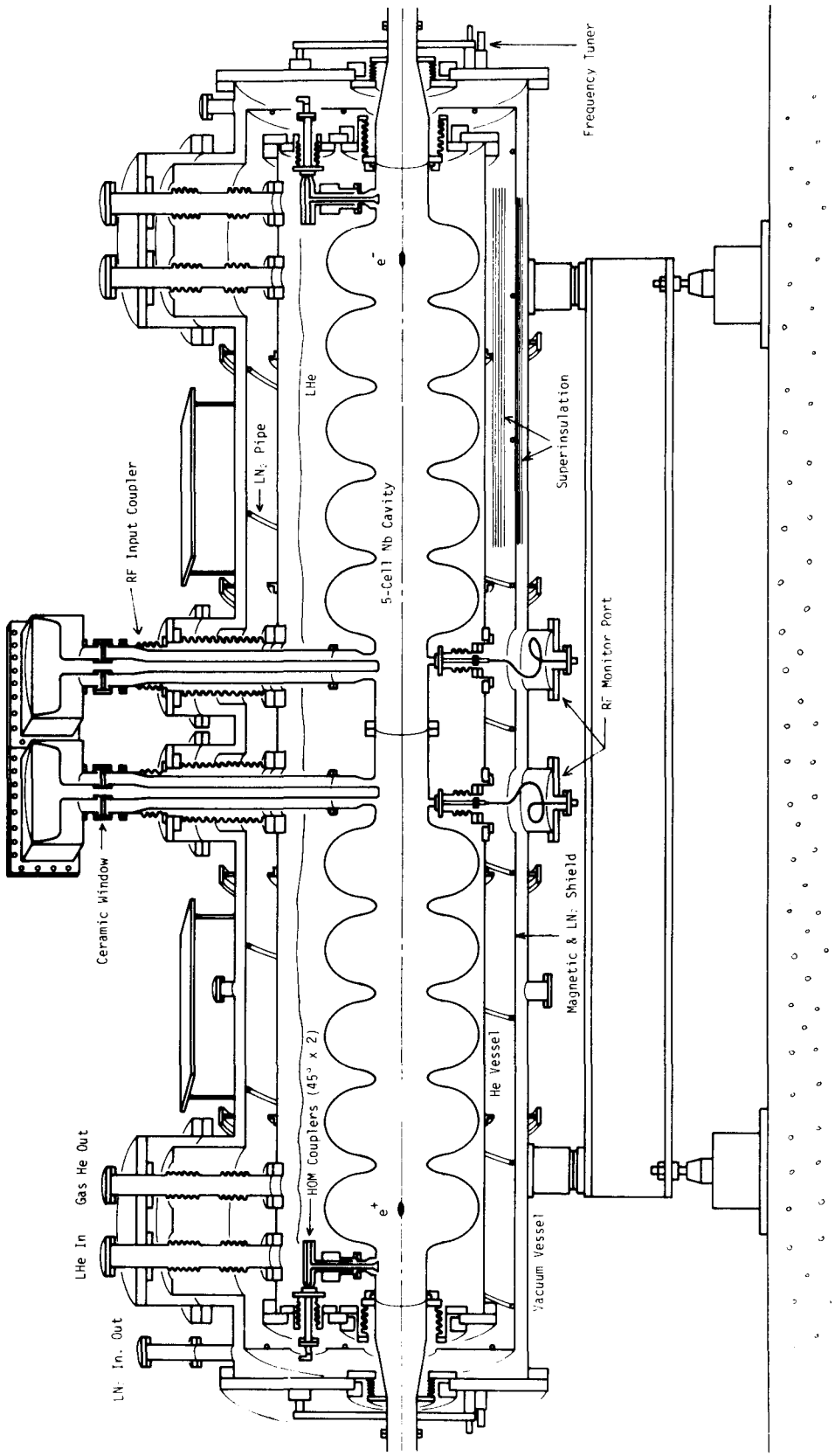

Fig. 12 MR Horizontal Cryostat.

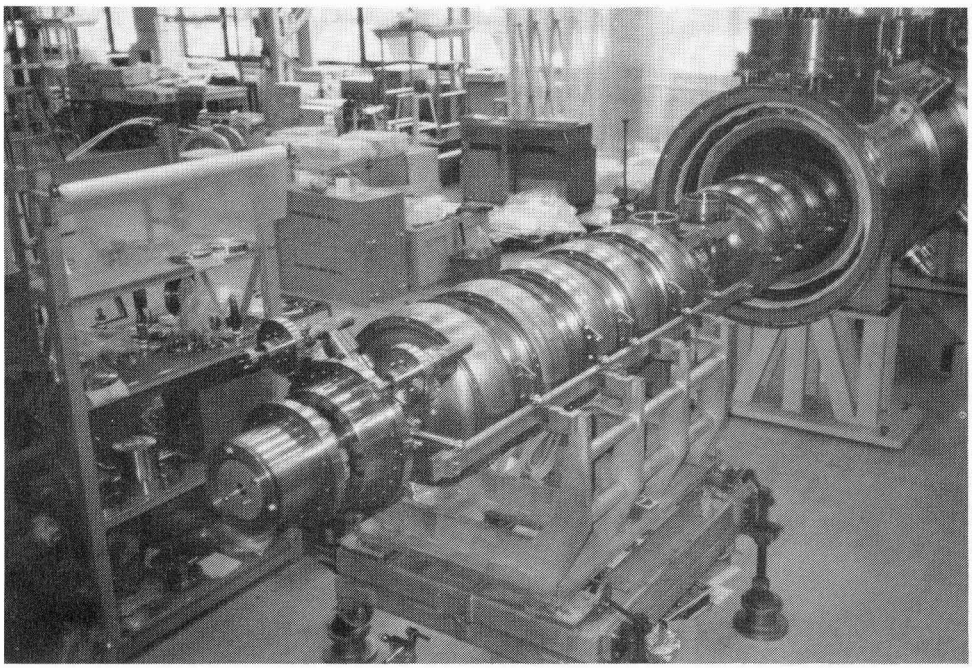

Photo. 2 Preassembling of the MR Cavities for Vacuum Leak Test.

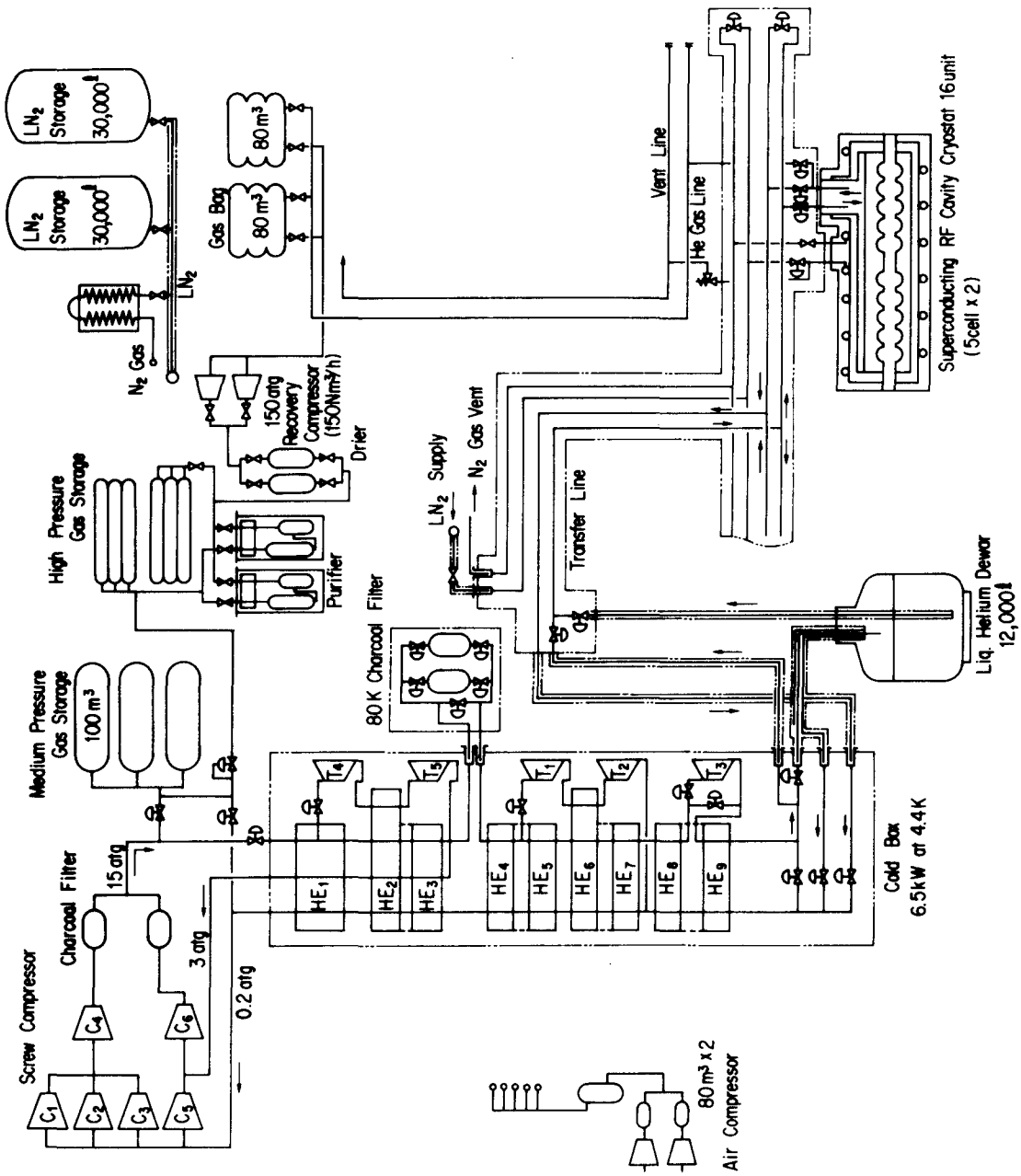

Fig. 13 Flow Diagram of the Refrigeration System.

5) Operation of two cavities and with the normal conducting system
6) Interlock system and effect of break down
7) Change of the performance in the environment of the actual storage ring

Now we are very busy and have many works to be done before the operation of the system of MR, but we are much encouraged by the good results of first two MR cavities.

Acknowledgement

We wish to thank Professors T. Nishikawa, S. Ozaki and Y. Kimura for their continuous encouragements, we are indebted to Professors H. Baba and E. Ezura for their suggestions in designing the RF system. We are very grateful to Messrs. U. Ishimaru, J. Miyasaka and T. Suzuki for their support to our work.

References

1) Y. Kimura, Proc. 13th Int. Conf. on High Energy Accelerators, Novosibirsk, (1986), KEK Preprint 86-50 (1986).
2) G. Horikoshi and Y. Kimura, Proc. 1987 Particle Accelerator Conf., Washington, (1987), KEK Preprint 87-23 (1987).
3) T. Higo et al., IEEE Trans. Nucl. Sci. NS-32, (1985) 2384.
4) E. Ezura et al., Proc. 1987 Particle Accelerator Conf., Washington, (1987), KEK Preprint 87-33 (1987).
5) Y. Kojima, Proc. 11th Int. Conf. on Cyclotrons and their Applications, Tokyo, (1986), KEK Preprint 86-67 (1986).
6) T. Furuya et al., Proc. 13th Int. Conf. High Energy Accelerators, Novosibirsk, (1986).
7) K. Hara et al., Proc. of the Cryog. Eng. Conf., Fermilab, (1987).
8) S. Noguchi et al., Proc. 5th Symp. on Accelerator Science and Technology, KEK (1984) 122.